23P166-B

Comparison of fluid behavior of implosion dynamics derived by difference of equation-of-state
状態方程式モデルの違いによる慣性核融合爆縮過程の流体挙動の比較

Yu Komatsu, Toru Sasaki, Takashi Kikuchi, Nob. Harada, Hideo Nagatomo[1)]
小松悠, 佐々木徹, 菊池崇志, 原田信弘, 長友英夫

Nagaoka University of Technology, Kamitomioka 1603-1, Nagaoka, Niigata, 940-2188, Japan
長岡技術科学大学　〒940-2188　新潟県長岡市上富岡町1603-1
[1)] *Institute of Laser Engineering, Osaka University, Yamadaoka 2-6, Suita, Osaka, 565-0871, Japan*
大阪大学レーザーエネルギー学研究センター　〒565-0871　大阪府吹田市山田丘2-6

Comparing hydrodynamic simulation with various equation of state (EOS), we obtained difference of EOS for implosion dynamics. To evaluate the implosion process, we used the two-dimensional radiation hydrodynamics simulation code with QEOS, ideal gas EOS, and SESAME. The maximum density for the ideal gas EOS is higher than that for the QEOS. The sound velocity of the SESAME is faster than that for the QEOS. These results indicated that each EOS model affected the implosion dynamics in inertial confinement fusion (ICF) .

1. Introduction

During the implosion process of ICF, the target material passes through a transition from solid to plasma. To generate inertial fusion energy, we should clearly understand the hydrodynamics of fuel pellet in wide density-temperature regime. The implosion dynamics is dominated by complex physical phenomena, such as strong shock wave, thermodynamics, atomic process, radiation transport, and so on. Recently, warm dense state, which is one of a thermodynamic regime defined by 0.01-1 times solid density with temperature of 0.1-10 eV, is pointed to the difference of existing equation-of-state models. The reason why the region includes the phase-transition from solid to plasma states, degenerated electrons, and coupled ions. To understand the effect on implosion dynamics with warm-dense-matter's EOS, we demonstrate to evaluate the changing implosion dynamics due to difference EOS models.

The purpose of this study is to compare to the fluid behavior of implosion dynamics for the various EOS models by numerical simulations.

2. Simulation code and EOS models

To evaluate the implosion process, we used the two-dimensional radiation hydrodynamics simulation code, PINOCO [1]. The EOS equipped in PINOCO is based on the quotidian EOS (QEOS) [2] with a fitting formula [3].

QEOS[2,3] and SESAME [4] are usually used numerical simulations of ICF. QEOS stands for quotidian equation of state. The cold and electron thermal property are based on semi-empirical bonding correction and the Thomas-Fermi model, respectively. The ion thermal properties evaluated with Cowan's model. Thermodynamic derivatives such as specific heat, sound speed can be easy to use from composed formulas.

SESAME is tabular data of the pressure and internal energy per unit mass as a function of temperature and density for each material [4]. The pressure and internal energy of SESAME should be interpolation of the finite number of data. Therefore, the thermodynamic derivatives should be careful due to discontinuity of models.

Figure 1 shows pressure curves at constant temperature. The pressure for ideal gas EOS is lower then that for QEOS and SESAME in a high density and low temperature regime. There is a difference in low temperature and near the solid density regime even if between QEOS and SESAME.

Spherical implosion of CH shell target was simulated. The thickness and radius of the shell are 6.8 μm and 241.2 μm. Background density and shell density are 1.0×10^{-6} g/cm^3 and 1.0 g/cm^3, respectively. To clarify the implosion dynamics from difference of EOS models, we neglect the radiation transport. The target is irradiated by uniform laser which energy and pulse width are 2.0 kJ and 1.0 ns with Gaussian, full width at half maximum (FWHM).

3. Results

Figure 2 shows the density profile for QEOS and ideal gas EOS in radial direction. The results

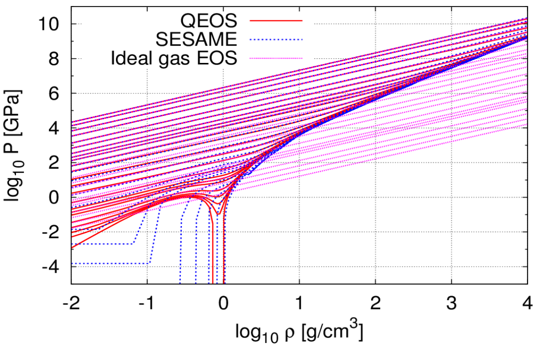

Fig. 1. Comparison of QEOS, ideal gas EOS, and SESAME pressure curves at constant temperature.

indicated that the implosion dynamics of both EOS cases are different structure around the shock front. Thus, from these time evolutions, the implosion velocity for the ideal gas EOS is faster than that for the QEOS. The difference of hydrodynamic structure is occurred by the degenerated pressure at over the solid density, which is $\log_{10} \rho \sim 0$ as shown in Fig. 1.

The maximum density for the ideal gas EOS is achieved 3560 g/cm^3 and that for the QEOS is obtained 741 g/cm^3.The compressibility κ is expressed as follows,

$$\kappa = \frac{1}{\rho}\left(\frac{\partial \rho}{\partial p}\right)_T = \frac{1}{\rho}\frac{1}{C_s}, \qquad (1)$$

where, ρ is the density, p is the pressure, and C_S is the sound velocity. Therefore, the EOS models affect the maximum density.

Figure 3 shows the density profile for QEOS and SESAME in radial direction. In the interior of shell, the shock velocity of SESAME is faster than that for QEOS. SESAME has Maxwell construction at warm dense regime, which is under the solid density. Thus, the propagation structure in interior of shell is quite different between both EOS models.

4. Conclusions

We investigated the implosion dynamics with the QEOS, ideal gas EOS, and SESAME by using PINOCO. The maximum density between QEOS and SESAME changed by the degenerated pressure. The propagation structure in interior of shell between QEOS and SESEAME changed by Maxwell construction at warm dense regime. Through these comparisons, we will construct the valuable EOS for ICF.

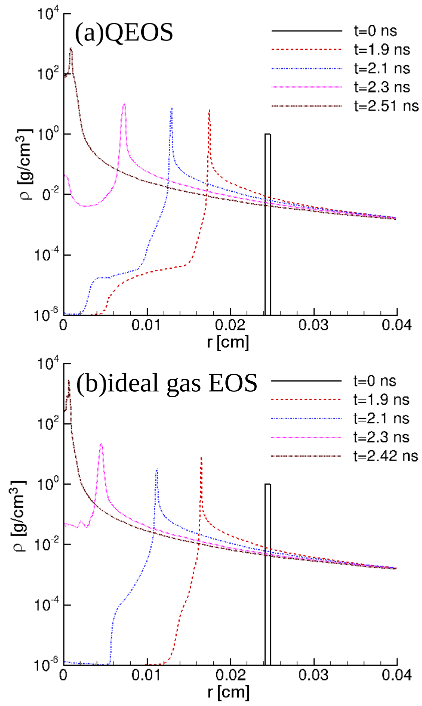

Fig. 2. Time-evolution of density profiles for radial direction. (a) QEOS and (b) ideal gas EOS. The solid line indicates the initial time of t=0 ns, the doted color lines denote 1.9 ns, 2.1 ns, and 2.3 ns, respectively. 2.51 ns for QEOS and 2.42 ns for ideal gas EOS show the maximum compression.

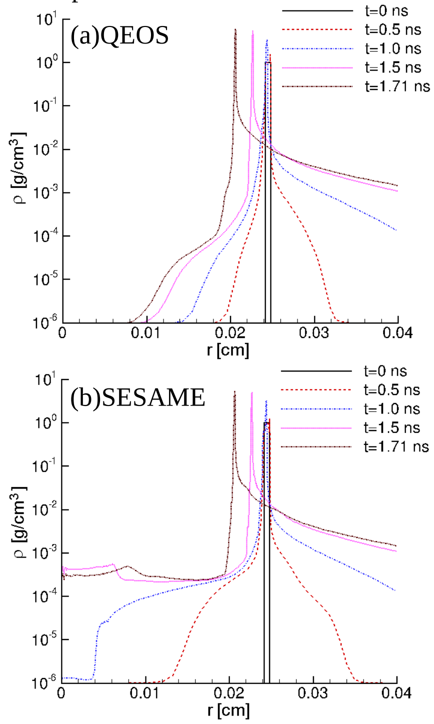

Fig. 3. Time-evolution of density profiles for radial direction. (a) QEOS and (b) SESAME. The solid line indicates the initial time of t=0 ns, the doted color lines denote 0.5 ns, 1.0 ns, 1.5 ns, and 1.71 ns, respectively.

References

[1] H. Nagatomo, et al., Phys. Plasmas **14**, (2007) 056303.

[2] R. M. More, et. al., Phys. Fluids **31**, (1988) 3059.

[3] K. Takami and H. Takabe, Technol. Rep. Osaka Univ. **40**, (1990) 159.

[4] S. P. Lyon, et al., Group T-1, LA-CP-98-100 (1988).